

## **OPEN ACCESS**

# Perspective—Reversible Magnesium Storage in Silicon: An Ongoing Challenge

To cite this article: Dongyang Zhang et al 2020 J. Electrochem. Soc. 167 050514

View the <u>article online</u> for updates and enhancements.





# Perspective—Reversible Magnesium Storage in Silicon: An Ongoing Challenge

Dongyang Zhang,<sup>1</sup> Jintao Fu,<sup>1,\*</sup> Zeyu Wang,<sup>1,3</sup> Lin Wang,<sup>1,\*</sup> John S. Corsi,<sup>1,2,\*</sup> and Eric Detsi<sup>1,2,\*\*,z</sup>

The increasing popularity of rechargeable commercial lithium-ion batteries raises a serious sustainability concern: Relying solely on lithium-ion batteries for the global portable/non-stationary electrochemical energy storage demands will put considerable strain on the resources used in these batteries. Therefore, alternative rechargeable battery technologies, including magnesium-ion batteries, are desirable. Silicon is very attractive for largescale application as a magnesium-ion battery anode due to its high natural abundance and its ultrahigh gravimetric capacity of  $3.816 \text{ mAh g}^{-1}$  for magnesium storage in the form of magnesium silicide (Mg<sub>2</sub>Si). Despite these unique advantages, to date the reversible electrochemical storage of magnesium in silicon has not yet been demonstrated experimentally, although theoretical studies predict that alloying reactions of silicon with magnesium are thermodynamically possible. The present article is aimed at elucidating the challenge and current status associated with the reversible storage of magnesium in silicon and presenting the future needs to overcome this challenge.

© 2020 The Author(s). Published on behalf of The Electrochemical Society by IOP Publishing Limited. This is an open access article distributed under the terms of the Creative Commons Attribution 4.0 License (CC BY, http://creativecommons.org/licenses/by/4.0/), which permits unrestricted reuse of the work in any medium, provided the original work is properly cited. [DOI: 10.1149/1945-7111/ab736b]

Manuscript submitted October 24, 2019; revised manuscript received December 24, 2019. Published February 21, 2020. This paper is part of the JES Focus Issue on Heterogeneous Functional Materials for Energy Conversion and Storage.

The rechargeable lithium-ion battery (LIB) technology has revolutionized the way we live, as recognized by the 2019 Nobel Prize in Chemistry. This revolution is now rapidly transforming the transportation industry as depicted by the myriad of battery electric vehicles on the market (e.g. Tesla, Nissan Leaf, Renault Zoe, BMW i3, Chevrolet Bolt EV, Ford Focus Electric, etc...). The widespread popularity of LIB-powered electric vehicles will directly contribute to mitigate our environmental issues, since gasoline-powered vehicles emit nearly one quarter of the U.S. greenhouse gases, making them one of the primary contributors to the global climate change. On the other hand, relying only on LIBs to power electric vehicles will put considerable strain on lithium, cobalt and nickel resources used in these batteries. 3-7 In fact, resources used in LIBs are becoming more expensive due to high demand, and the global cobalt market heavily depends on supplies from countries with high geopolitical risks. 6-11 Therefore, alternative battery technologies other than LIBs are desirable to satisfy our growing demand for energy. Magnesium-ion batteries (MIBs) offer many distinct advantages over LIBs, including the abundance of magnesium, the reversible dendrite-free deposition of magnesium, <sup>4,12–15</sup> the divalent nature of the magnesium ion, the relatively smaller ionic radius of magnesium ions compared to lithium ions, and finally the fact that magnesium metal is less reactive and thus safer than lithium metal. 14,16–20 Despite these advantages, magnesium metal is not used as the anode in practical MIBs due to its incompatibility with conventional battery electrolytes. 13,21-24 As a consequence, instead of magnesium metal, alloys of magnesium are used as the anode in MIBs,  $^{3,25-27}$  among which Mg<sub>3</sub>Bi<sub>2</sub> (capacity: 385 mAh g<sup>-1</sup>),  $^{26}$  Mg<sub>2</sub>Sn (capacity 903 mAh g<sup>-1</sup>),  $^{2,28}$  Mg<sub>2</sub>Ga<sub>5</sub> (capacity: 308 mAh g<sup>-1</sup>)<sup>11</sup> are the most promising candidates. With the exception of Mg<sub>2</sub>Sn, commonly investigated alloy-type MIB anodes exhibit a relatively low gravimetric capacity; for new applications such as the above-mentioned battery electric vehicles, high capacity anodes are desirable to reduce the overall mass of the battery without lowering its specific energy density.

Silicon-magnesium and silicon-lithium alloys including Mg<sub>2</sub>Si and Li<sub>22</sub>Si<sub>5</sub> are very attractive as magnesium-ion and lithium-ion battery anodes, due to the high natural abundance of silicon (Si is the 2nd most abundant element in the Earth's crust) and its ultrahigh theoretical gravimetric capacity for magnesium storage (3,816 mAh g<sup>-1</sup> for the Mg<sub>2</sub>Si phase) and for lithium storage (4,200 mAh g<sup>-1</sup> for Li<sub>22</sub>Si<sub>5</sub> phase). For the sake of comparison, the theoretical capacity of graphite used in commercial LIBs is only 372 mAh g<sup>-1</sup>, which is roughly one order of magnitude lower than that of silicon. Magnesium and lithium storage in silicon is a diffusion-controlled process, which is extremely sluggish in bulk materials. Therefore, nanoscale silicon instead of bulk silicon is needed to shorten the effective diffusion distance of magnesium and lithium in these host materials.<sup>29-35</sup> Although various types of nanostructured silicon (nano-Si) including silicon nanoparticles, 36–38 silicon nanowires, 33,39,40 and nanoporous silicon, 29,34,41 have been processed and successfully used as the anodes in LIBs, <sup>29–34</sup> to date, the reversible electrochemical storage of magnesium in nano-Si has not yet been demonstrated experimentally, although theoretical studies predict that alloying reactions of silicon with magnesium are thermodynamically favorable.<sup>35</sup> In the *Current Status* section of this article, we elucidate the main challenge and current progress associated with the reversible storage of magnesium in silicon; and in the Future Needs and Prospects section, we suggest a possible approach to overcome this challenge.

#### **Current Status**

The reversible storage of magnesium in alloy-type anodes including  $Mg_3Bi_2^{\ 26}\ Mg_2Sn$ ,  $^{2,28,42}\ Mg_2Ga_5$ ,  $^{11}$  and  $Mg_2Si$  is governed by mass transport, which involves the solid-state diffusion of Mg ions in or out of the host material (Bi, Sn, Ga and Si). The diffusion of Mg ions in the bulk of the material is extremely sluggish because of its divalent nature, which results in much stronger electrostatic interactions with the lattice of the host material compared with similar electrostatic interactions in the case of monovalent lithium ions. Nanostructured materials  $^{2,26,28,42}$  and solid-liquid phase changing materials  $^{11}$  have been proposed to mitigate this issue. In practice, the diffusivity of magnesium in nanostructured host materials is significantly affected by two factors: The native oxide

<sup>&</sup>lt;sup>1</sup>Department of Materials Science & Engineering, University of Pennsylvania, Philadelphia, Pennsylvania 19104-6272, United States of America

<sup>&</sup>lt;sup>2</sup>Vagelos Institute for Energy Science and Technology (VIEST), Philadelphia, Pennsylvania 19104, United States of America <sup>3</sup>State Key Laboratory of Advanced Welding and Joining, Harbin Institute of Technology, Harbin 150001, People's Republic of China

<sup>\*</sup>Electrochemical Society Student Member.

<sup>\*\*</sup>Electrochemical Society Member.

<sup>&</sup>lt;sup>z</sup>E-mail: detsi@seas.upenn.edu

or interfacial passive film surrounding the nanostructured material and the characteristic size of this nanostructured material:

- In the former case, the presence of a native oxide or any other type of surface passive film at the interface of nanostructured materials is usually unavoidable, since these surface films automatically form whenever a reactive nanostructured material is exposed to air and moisture during its processing and handling. 43-47 In the case of silicon for instance, exposed nano-Si will readily react to form a passive native silicon oxide (SiO<sub>2</sub>) film. 43-47 which may result in a core-shell structure, as illustrated in Fig. 1a where the nano-Si (yellow) is surrounded by a passive SiO<sub>2</sub> shell (grey). Such a SiO<sub>2</sub> shell is usually not problematic in lithium-ion battery anodes because monovalent lithium ions can react with SiO<sub>2</sub> during the first cycle and "destroy" it through a conversion reaction, during which this SiO<sub>2</sub> is transformed into pure Si and Li<sub>2</sub>O. <sup>48</sup> In the case of MIBs however, the diffusivity of divalent magnesium ions through such passive films is highly unfavorable, due to the strong electrostatic interaction between the divalent magnesium ions and electronic charges in the lattice of the passive film. 17,49 Thus, in contrast to LIB anodes in which the passive surface film is converted into the corresponding metal or metalloid and Li<sub>2</sub>O, passivating surface films are fatal in MIB anodes.
- (2) In the latter case, since magnesium storage in the bulk of nanostructured materials involves solid-state diffusion, the characteristic size of these nanostructured materials is critical. For the sake of illustration, while it can take up to ~3 weeks to store magnesium in commercial Sn nanoparticles with average particle size in the range of 150 nm,² this time is significantly reduced to a few hours, if the characteristic size of nanostructured Sn is in the sub-50 nm range.²8,50,51 In fact, it has been reported that the critical size of nanostructured Sn should be below ~50 nm, for magnesium storage to occur at practical rates.²8,50 Obviously, such a critical upper size limit also exists in nano-Si, but the value has not yet been investigated, to our knowledge.

The issues described in (1) and (2) pertaining to the blocking surface oxide and the critical structure size represent the fundamental challenges that impede the reversible storage of magnesium in silicon. Note that the huge volume changes that occur during charge storage in alloy-type anodes are not discussed in this article, since these volume changes are not critical for the problem addressed in this article, namely the difficulty to reversibly store

magnesium in silicon. Instead, these volume changes are critical for the cycling stability of battery electrodes. The current state-of-the-art solution to overcome these two issues involves the use of nearly "oxide-free" nano-Si as the anode in MIBs. The same solution has been successfully demonstrated in Sn, where various in situ synthesis strategies have been used to produce nearly oxide-free nanostructured Sn directly inside the battery cell. For example, Parent et al.,<sup>51</sup> as well as Chen et al.,<sup>50</sup> used the SnSb alloy as the anode in MIB and took advantage of the phase separation of SnSb into Sn-rich and Sb-rich phases during cycling to produce nanostructured Sn embedded in the Sb matrix. 50,51 This in situ generated nanostructured Sn was obviously nearly oxide-free, since during cycling the electrode materials were not exposed to any external environment other than the anhydrous battery organic electrolyte. These authors further observed that the critical size of nanostructured Sn for which magnesium storage is kinetically acceptable was in the range of  $\sim$ 33  $\pm$  20 nm. <sup>50,51</sup> One issue when nanostructured Sn is produced in situ from the phase separation in the SnSb alloy is that the Sb-rich phase cannot store magnesium. This Sb phase is considered "dead" mass in the battery, which is undesirable. To avoid this dead mass issue, Detsi and co-workers proposed the airfree in situ processing of nanostructured Sn directly from bulk Mg<sub>2</sub>Sn. <sup>28,42</sup> In their process, micrometer-sized bulk Mg<sub>2</sub>Sn was used as the active material in a MIB half-cell; during the cycling magnesium was removed from Mg<sub>2</sub>Sn (and plated onto the counter electrode), resulting in the formation of nanostructured Sn. <sup>28,42</sup> Here also, the nanostructured Sn produced under these conditions was nearly oxide-free, since the materials were sealed in the battery cell under argon atmosphere with 0.1 ppm of O<sub>2</sub> and 0.1 ppm of H<sub>2</sub>O.<sup>28</sup> The characteristic structure size for which magnesium storage took place at acceptable rates was also found to be in the range of sub-50 nm.<sup>28</sup> These examples illustrate how the issues raised in (1) and (2) were overcome in the case of Sn. A straightforward question is the applicability of the air-free in situ processing strategy to nanostructured silicon. In order words, is it possible to produce nearly oxide-free nano-Si from micrometer-sized bulk Mg<sub>2</sub>Si directly inside the battery cell as illustrated Fig. 1b where the starting Mg<sub>2</sub>Si (blue) is decomposed into oxide-free nano-Si (yellow) during the first demagnesiation step, and subsequently use this oxide-free nano-Si for reversible magnesium storage?

In order to answer the above question, we made nanostructured Si through air-free selective electrochemical removal of Mg from bulk Mg<sub>2</sub>Si parent material with characteristic particle size in the range between 1–10  $\mu$ m, using a magnesium-ion battery half-cell configuration with the Mg<sub>2</sub>Si parent material as the working

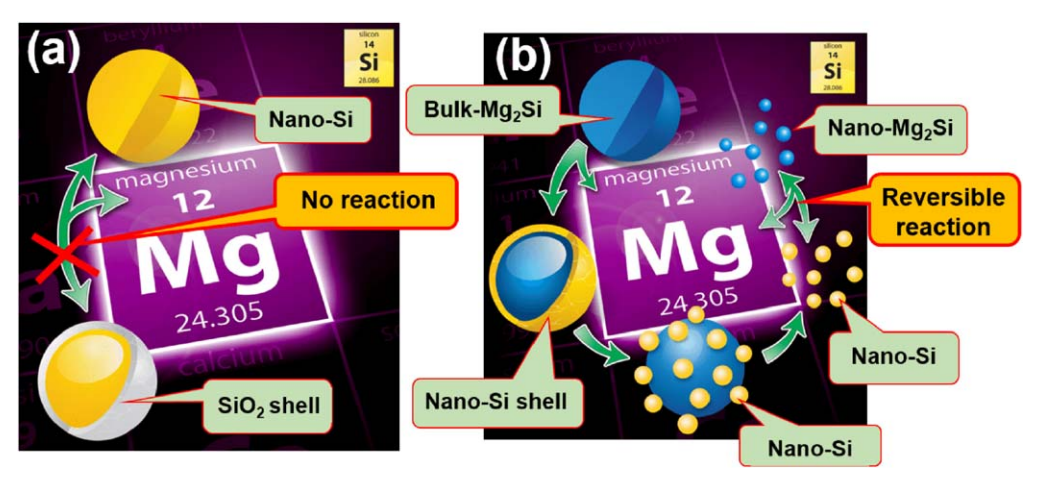


**Figure 1.** Graphical overview of the issues involving magnesium storage in silicon. (a) The yellow particle represents a nano-Si particle covered with its native oxide  $-SiO_2$  (the grey  $SiO_2$  shell around the yellow nano-Si core) used as magnesium-ion battery anode. The  $SiO_2$  shell restricts Mg storage in nano-Si. (b) Instead of using nano-Si coated with its native oxide as magnesium-ion battery anode, one can use micrometer-sized bulk parent materials illustrated by the blue Mg<sub>2</sub>Si particle. A bulk Mg<sub>2</sub>Si particle will be converted into nano-Si inside the battery cell when the cell is operating (i.e. in situ processing), as depicted by the yellow nano-Si shell around the blue and yellow Si nanoparticle. In this manner, the freshly made nano-Si is nearly oxide-free since the cell operates under inert environment.

electrode (the working electrode is made using a standard battery electrode slurry protocol<sup>28</sup>), Mg metal as the counter and reference electrodes, and all-phenyl complex (APC) as the electrolyte. The first demagnesiation curve of Mg<sub>2</sub>Si is shown in Fig. 2a. This demagnesiation occurs at a relatively high potential (>1.2 V vs Mg/Mg<sup>2+</sup>) compared with the potential associated with the first demagnesiation curve of  $Mg_2Sn$  (>0.35 V vs  $Mg/Mg^{2+}$ ) from our previous work.<sup>28</sup> Thermodynamically, (de)magnesiation of Mg<sub>2</sub>Si and Mg<sub>2</sub>Sn should occur around 0.1–0.2 V vs Mg/Mg<sup>2+</sup>.<sup>35,52</sup> This means that the high demagnesiation potential of  $\sim 1.2$  V vs Mg/Mg<sup>2+</sup> recorded in Mg<sub>2</sub>Si obviously suggests that Mg removal from Mg<sub>2</sub>Si is much more difficult than Mg removal from Mg<sub>2</sub>Sn, and requires a very high overpotential. Note that in the case of Sn, the relatively high overpotential is only present during the first demagnesiation step, since most of the nanostructured materials are produced during the first cycle.<sup>28</sup> Similarly, in the case of Si, we do not expect high overpotentials to occur during the subsequent cycles that will follow the first demagnesiation step. It is worth mentioning that when demagnesiation results in the formation of a liquid phase anode from a solid phase (i.e. solid-liquid phase transition), the high overpotential is not present during the first demagnesiation step, as demonstrated in our recent work in the case Mg<sub>2</sub>Ga<sub>5</sub>.

The capacity achieved in  $Mg_2Si$  during the first demagnesiation step is approximately 3,500 mAh  $g^{-1}$  (see Fig. 2a), which represents  $\sim 91.7\%$  of the theoretical gravimetric capacity of  $Mg_2Si$ , namely 3,816 mAh  $g^{-1}$ . This capacity value suggests that roughly 91.7% of the starting  $Mg_2Si$  has been converted into nano-Si, which is much higher than the conversion yield of  $\sim 70\%$  achieved in  $Mg_2Si$  (i.e.  $\sim 70\%$  of the starting  $Mg_2Si$ n was converted into nanostructured Sn in our previous works<sup>28</sup>).

The typical diffraction patterns of the Mg<sub>2</sub>Si composite slurry electrode cast onto a copper foil substrate/current collector are shown in Fig. 2b before (black) and after (red) magnesium removal. The black pattern of the pristine Mg<sub>2</sub>Si composite slurry electrode

matches well with the characteristic peaks of carbon (ICDD PDF No. 41-1487) marked by green vertical bars, Mg<sub>2</sub>Si (ICDD PDF No. 35-0773) marked by blue vertical bars as well as copper (ICDD PDF No. 04-0836) marked by pink vertical bars. Note that the carbon peak located at  $\sim 26.4^{\circ}$  comes from the carbon materials used as conductive additives in the slurry. The peaks of Cu come from the copper foil used as the current collector/substrate. By comparison, the red pattern of the electrode after the first demagnesiation illustrates the disappearance of Mg<sub>2</sub>Si peaks with no emergence of new characteristic peaks, which suggests that the pristine Mg<sub>2</sub>Si composite slurry has been considerably demagnesiated and converted into nanostructured Si during this process. It is worth noting that the absence of Si peaks in the red pattern of the demagnesiated nano-Si suggests that the corresponding nano-Si is amorphous, which is not unusual in Si-based battery anodes. Indeed, the transformation of crystalline Si into amorphous Si during electrochemical cycling also occurs in Li-ion battery anodes.

The typical scanning electron micrographs of the  $Mg_2Si$  particles before and after magnesium removal are shown in Figs. 2c and 2d, respectively, combined with the corresponding chemical composition in the insets, obtained from Energy-dispersive X-ray spectroscopy (EDS). The signal intensity difference depicted from the insets indicates a significant amount of Mg removal from  $Mg_2Si$  after the first demagnesiation. Besides, it can be seen that after demagnesiation, nanostructured Si with characteristic size of  $\sim 100$  nm is formed (Fig. 2d). Al and Cl signals observed on the EDS spectrum after demagnesiation (inset Fig. 2d) come from the residual APC electrolyte, trapped in the pores of the fabricated nanostructured Si. Surface characterization techniques including XPS analysis will be performed in the future to further investigate the surface state of the demagnesiated material.

The chemical composition of the Mg<sub>2</sub>Si composite electrode was further investigated using EDS elemental mapping. Representative EDS maps before and after demagnesiation are shown in Figs. 3a

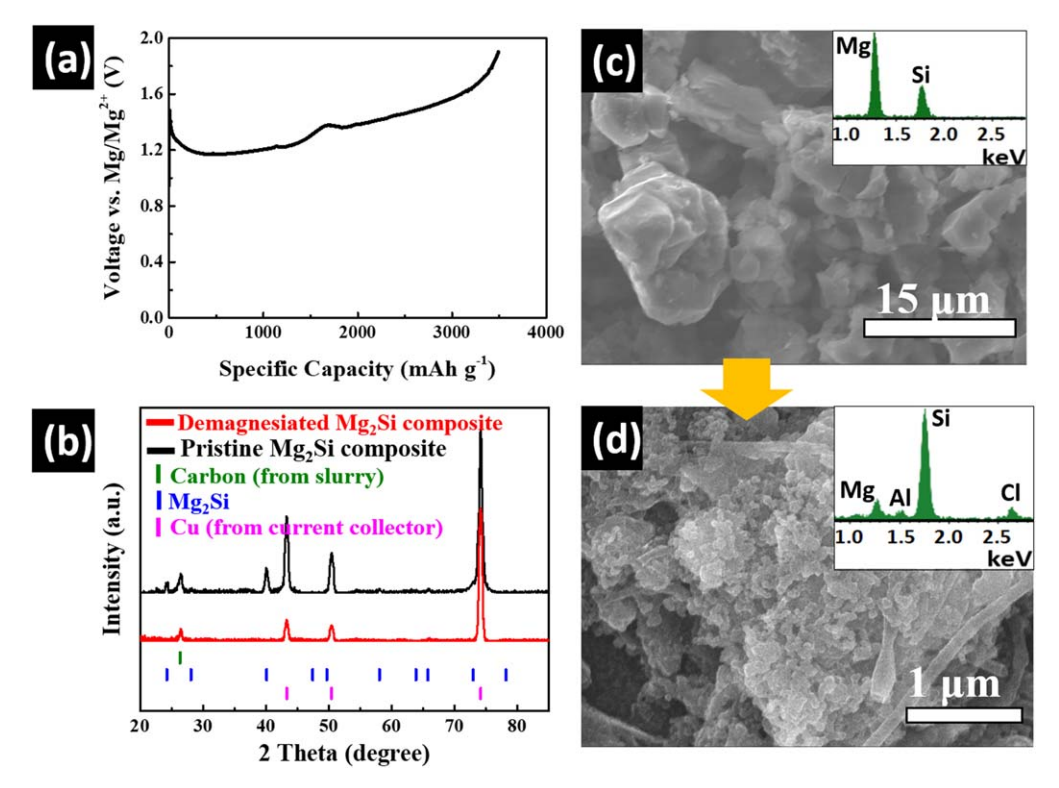


Figure 2. (a) First demagnesiation curve of  $Mg_2Si$  electrode at the C-rate of C/50. The corresponding gravimetric capacity is  $\sim 3,500$  mAh  $g^{-1}$ , indicating that  $\sim 91.7\%$  of the pristine  $Mg_2Si$  has been converted into nano-Si after the first demagnesiation step. (b) XRD patterns of the  $Mg_2Si$  electrode before (marked in black) and after (marked in red) the first demagnesiation step. The difference between the patterns before and after the first demagnesiation demonstrates the phase transformation from  $Mg_2Si$  to nano-Si, which became amorphous after demagnesiation. Scanning electron microscope images and EDS spectra of the  $Mg_2Si$  electrode before (c) and after (d) the first demagnesiation step. It can be seen that nearly all Mg has been removed from the pristine  $Mg_2Si$ , and that nanostructured Si with average feature size in the range of  $\sim 100$  nm has been created after demagnesiation.

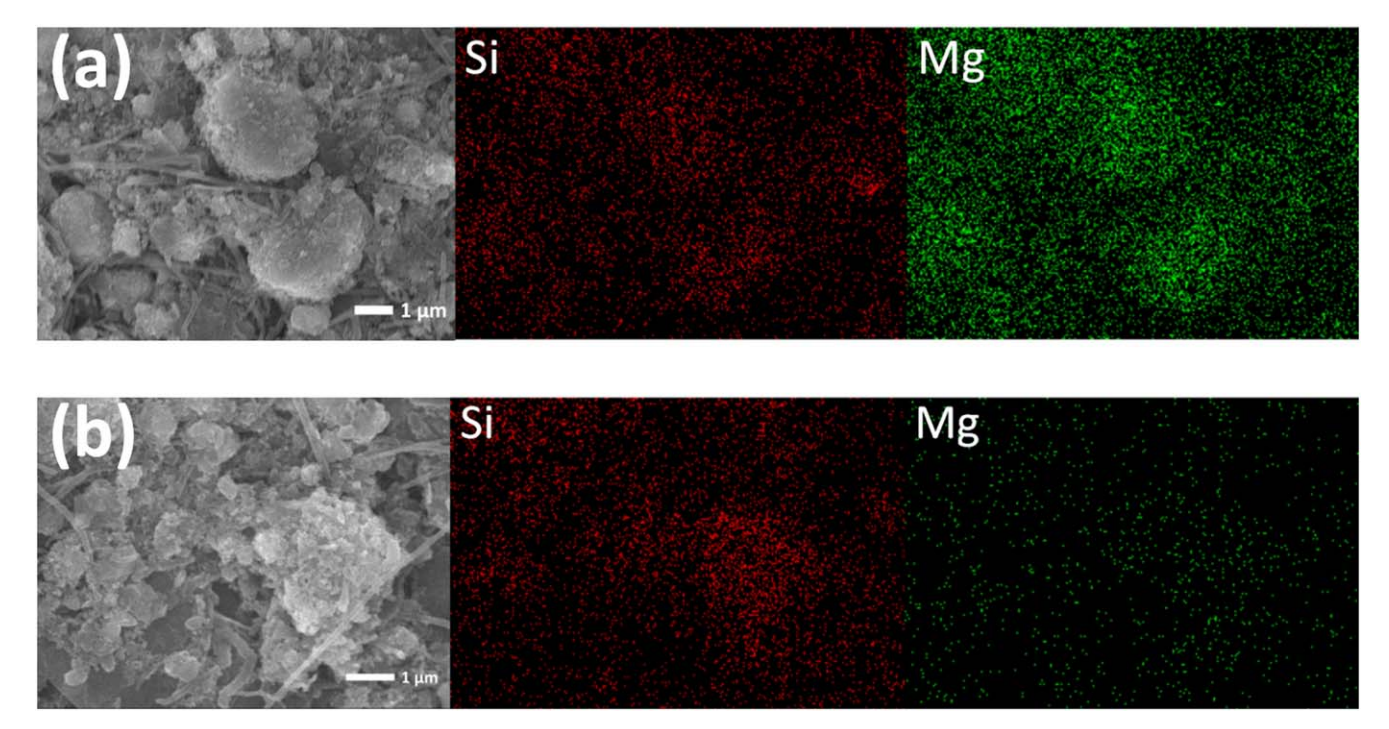


Figure 3. EDS elemental mapping of (a) pristine Mg<sub>2</sub>Si particles and (b) demagnesiated Mg<sub>2</sub>Si particles. For pristine Mg<sub>2</sub>Si, the distribution of Si (red) and Mg (green) elements are uniform across the particles, while in the demagnesiated Mg<sub>2</sub>Si, the particles almost fully consist of Si with minor remaining Mg element.

and 3b, respectively. In the pristine  $Mg_2Si$  sample with micron-range particles (Fig. 3a), the distribution of elemental Mg (characterized in green) and Si (characterized in red) across the particles were uniform and chemically indistinguishable. After demagnesiation (Fig. 3b), however, the particles almost fully consist of only Si, with only minor Mg signal detected. This agrees with the above-mentioned result that roughly 91.7% of Mg has been removed during demagnesiation while 8.3% of Mg were still in the particles.

## **Future Needs and Prospects**

Unfortunately, despite the successful electrochemical demagnesiation of bulk Mg<sub>2</sub>Si into nearly oxide-free nanostructured Si with feature size in the range of  $\sim 100$  nm, attempts to subsequently reverse the process by electrochemically magnesiating these nanostructured Si were unsuccessful. Thus, based on the current status, it is possible to electrochemically remove magnesium from Mg<sub>2</sub>Si, but not to electrochemically introduce magnesium into oxide-free nanostructured silicon with feature size of ~100 nm. Knowing that the critical size for reversible Mg storage in oxide-free nanostructured Sn was reported to be in the range of  $\sim$ 30-50 nm, <sup>28,50,51</sup> we believe that the failure to store magnesium back in the oxide-free nano-Si is explained by the relative large structure size  $\sim$ 100 nm of this nano-Si. Therefore, the future needs in the field are: (i) Identifying the critical structure size of Si for which Mg storage can reversibly take place at acceptable rates. This will require both computational simulations and experimental works for validation. (ii) Finding ways to process oxide-free nanostructured Si with size below this critical value, and to demonstrate the reversible storage of Mg in Si.

#### **Summary**

Various efforts to develop MIB anodes have demonstrated the successful storage of Mg in materials such as Bi, Sn, Ga, during which  $Mg_3Bi_2$ ,  $Mg_2Sn$ , and  $Mg_2Ga_5$ , are reversibly formed, respectively. However, to date Mg storage in Si—an ultrahigh-capacity anode material—to reversibly form  $Mg_2Si$ , has not yet been experimentally demonstrated. In this perspective article, the ongoing

challenges and progress associated with the reversible storage of Mg in Si are elucidated. To further illustrate the issues, we present our work in which micrometer-sized bulk Mg<sub>2</sub>Si is successfully demagnesiated into nearly oxide-free nanostructured Si with characteristic size around 100 nm; however, Mg could not be introduced back into these nanostructured Si to form Mg2Si. It is believed that the difficulty to introduce Mg in our oxide-free nanostructured Si is due to its characteristic size being larger than the critical size required for effective magnesiation. From these results, we highlight two important steps in developing a Si MIB anode: (1) The identification of the critical nanostructure size for magnesiation of Si and (2) the development of effective processing routes to synthesize nearly oxide-free nanostructured Si with characteristic size smaller than this critical value. A successful demonstration of an ultrahigh-capacity Si MIB anode will represent a significant step toward the development of high energy density MIBs as an alternative to LIBs.

#### Acknowledgments

The authors are thankful to Penn Engineering, the Vagelos Institute for Energy Science and Technology (VIEST), and the National Science Foundation (NSF) for their financial supports through the PI startup, the 2018 VIEST seed grant, and the NSF EAGER grant (CMMI-1840672), respectively. This work was carried out in part at the Singh Center for Nanotechnology, part of the National Nanotechnology Coordinated Infrastructure Program, which was supported by the NSF grant NNCI-1542153.

#### References

- 1. NobelPrize.org., Nobel Media AB (Published News) (2019).
- 2. M. Desai and R. P. Harvey, Fed. Regist., 82, 10767 (2017).
- N. Singh, T. S. Arthur, C. Ling, M. Matsui, and F. Mizuno, *Chem. Commun.*, 49, 149 (2013).
- D. Aurbach, Z. Lu, A. Schechter, Y. Gofer, H. Gizbar, R. Turgeman, Y. Cohen, M. Moshkovich, and E. Levi, *Nature*, 407, 724 (2000).
- J. M. Tarascon and M. Armand, Materials for Sustainable Energy: A Collection of Peer-Reviewed Research and Review Articles from Nature Publishing Group, 414, 171 (2010).
- 6. X. B. Cheng and Q. Zhang, J. Mater. Chem. A, 3, 7207 (2015).
- Z. Yang, J. Zhang, M. Kintner-Meyer, X. Lu, D. Choi, J. Lemmon, and J. Liu, *Chem. Rev.*, 111, 3577 (2011).

- 8. T. S. Arthur, N. Singh, and M. Matsui, Electrochem. Commun., 16, 103 (2012).
- 9. D. Aurbach, B. Markovsky, I. Weissman, E. Levi, and Y. Ein-Eli, ChemInform, 32 (2010).
- 10 P. Simon and Y. Gogotsi. Nature Mater. 7, 845 (2008).
- 11. L. Wang, S. S. Welborn, H. Kumar, M. Li, Z. Wang, V. B. Shenoy, and E. Detsi, Adv. Energy Mater., 9, 1902086 (2019).
- H. Tian et al., Nat. Commun., 8, 1 (2017).
  H. D. Yoo, I. Shterenberg, Y. Gofer, G. Gershinsky, N. Pour, and D. Aurbach, Energy Environ. Sci., 6, 2265 (2013).
- 14. N. Singh, T. Arthur, O. Tutusaus, J. Li, K. Kisslinger, H. Xin, E. Stach, X. Fan, and R. Mohtadi, ACS Appl. Energy Mater., 1, 4651 (2018)
- 15. M. Matsui, J. Power Sources, 196, 7048 (2011).
- 16. J. Muldoon, C. B. Bucur, and T. Gregory, Chem. Rev., 114, 11683 (2014).
- 17. R. Mohtadi and F. Mizuno, Beilstein J. Nanotechnol., 5, 1291 (2014).
- 18. O. Tutusaus, R. Mohtadi, N. Singh, T. S. Arthur, and F. Mizuno, ACS Energy Lett., **2**, 224 (2017).
- 19. Y. Cao, L. Xiao, W. Wang, D. Choi, Z. Nie, J. Yu, L. V. Saraf, Z. Yang, and J. Liu, Adv. Mater., 23, 3155 (2011).
- 20. C. F. Lopez, J. A. Jeevarajan, and P. P. Mukherjeea, J. Electrochem. Soc., 162, A2163 (2015).
- 21. J. Muldoon, C. B. Bucur, A. G. Oliver, T. Sugimoto, M. Matsui, H. S. Kim, G. D. Allred, J. Zajicek, and Y. Kotani, Energy Environ. Sci., 5, 5941 (2012).
- 22. E. M. Erickson, E. Markevich, G. Salitra, D. Sharon, D. Hirshberg, E. de la Llave, I. Shterenberg, A. Rosenman, A. Frimer, and D. Aurbach, J. Electrochem. Soc., 162, A2424 (2015).
- 23. N. Wu, Y. C. Lyu, R. J. Xiao, X. Yu, Y. X. Yin, X. Q. Yang, H. Li, L. Gu, and Y. G. Guo, NPG Asia Mater., 6, e120 (2014).
- 24. J. Song, E. Sahadeo, M. Noked, and S. B. Lee, J. Phys. Chem. Lett., 7, 1736 (2016).
- 25. Z. Liu, J. Lee, G. Xiang, H. F. Glass, E. N. Keyzer, S. E. Dutton, and C. P. Grey, Chem. Commun., 53, 743 (2017).
- 26. Y. Shao et al., Nano Lett., 14, 255 (2014).
- 27. J. Niu, H. Gao, W. Ma, F. Luo, K. Yin, Z. Peng, and Z. Zhang, *Energy Storage* Mater., 14, 351 (2018).
- 28. H. Yaghoobnejad Asl, J. Fu, H. Kumar, S. S. Welborn, V. B. Shenoy, and E. Detsi, Chem. Mater., 30, 1815 (2018).
- 29. J. B. Cook, H.-S. Kim, T. C. Lin, S. Robbennolt, E. Detsi, B. Dunn, and S. H. Tolbert, ACS Appl. Mater. Interfaces, 9, 19063 (2017).
- 30. M. H. Park, M. G. Kim, J. Joo, K. Kim, J. Kim, S. Ahn, Y. Cui, and J. Cho, Nano Lett., 9, 3844 (2009).
- 31. N. Nitta and G. Yushin, Part. Part. Syst. Charact., 31, 317 (2014)
- 32. Y. Zhao, X. Liu, H. Li, T. Zhai, and H. Zhou, Chem. Commun., 48, 5079 (2012).

- 33. C. K. Chan, H. Peng, G. Liu, K. McIlwrath, X. F. Zhang, R. A. Huggins, and Y. Cui, Nat. Nanotechnol., 3, 31 (2007).
- 34. T. Wada, J. Yamada, and H. Kato, J. Power Sources, 306, 8 (2016).
- 35. F. Legrain, O. I. Malyi, and S. Manzhos, Comput. Mater. Sci., 94, 214 (2014).
- Y. M. Lin, K. C. Klavetter, P. R. Abel, N. C. Davy, J. L. Snider, A. Heller, and C. B. Mullins, Chem. Commun., 48, 7268 (2012).
- 37. J. K. Lee, K. B. Smith, C. M. Hayner, and H. H. Kung, Chem. Commun., 46, 2025 (2010).
- 38. M. T. McDowell, I. Ryu, S. W. Lee, C. Wang, W. D. Nix, and Y. Cui, Adv. Mater., 24, 6034 (2012).
- 39. S. Chang, J. Moon, K. Cho, and M. Cho, Comput. Mater. Sci., 98, 99 (2015).
- 40. A. M. Chockla, J. T. Harris, V. A. Akhavan, T. D. Bogart, V. C. Holmberg, C. Steinhagen, C. B. Mullins, K. J. Stevenson, and B. A. Korgel, J. Am. Chem. Soc., 133, 20914 (2011)
- 41. W. Chen, Z. Fan, A. Dhanabalan, C. Chen, and C. Wang, J. Electrochem. Soc., 158, A1055 (2011).
- 42. Z. Wang, A. Bandyopadhyay, H. Kumar, M. Li, A. Venkatakrishnan, V. B. Shenoy, and E. Detsi, J. Energy Storage, 23, 195 (2019).
- 43. M. Morita, T. Ohmi, E. Hasegawa, M. Kawakami, and M. Ohwada, J. Appl. Phys., 68, 1272 (1990).
- 44. S. I. Raider, R. Flitsch, and M. J. Palmer, J. Electrochem. Soc., 122, 413 (1975).
- 45. D. Stiévenard and B. Legrand, Prog. Surf. Sci., 81, 112 (2006).
- 46. F. Li and M. K. Balazs, 21st Annu. Semicond. Pure Water Chem. Conf. (SPWCC), St. Clara, Ca1 (2002).
- 47. B. J. Winters, J. Holm, and J. T. Roberts, J. Nanoparticle Res., 13, 5473 (2011).
- 48. N. Yan, F. Wang, H. Zhong, Y. Li, Y. Wang, L. Hu, and Q. Chen, Sci. Rep., 3, 1568 (2013).
- 49. P. Saha, M. K. Datta, O. I. Velikokhatnyi, A. Manivannan, D. Alman, and P. N. Kumta, *Prog. Mater Sci.*, **66**, 1 (2014).
- 50. L. R. Parent, Y. Cheng, P. V. Sushko, Y. Shao, J. Liu, C. M. Wang, and N. D. Browning, Nano Lett., 15, 1177 (2015).
- 51. Y. Cheng, Y. Shao, L. R. Parent, M. L. Sushko, G. Li, P. V. Sushko, N. D. Browning, C. Wang, and J. Liu, Adv. Mater., 27, 6598 (2015).
- 52. O. I. Malyi, T. L. Tan, and S. Manzhos, J. Power Sources, 233, 341 (2013).
- 53. F. Murgia, E. T. Weldekidan, L. Stievano, L. Monconduit, and R. Berthelot, Electrochem, Commun., 60, 56 (2015).
- 54. Y. Han, N. Lin, T. Xu, T. Li, J. Tian, Y. Zhu, and Y. Qian, Nanoscale, 10, 3153 (2018).
- 55. J. W. Wang et al., Nano Lett., 13, 709 (2013).
- 56. N. Kim, S. Chae, J. Ma, M. Ko, and J. Cho, Nat. Commun., 8, 1 (2017).
- 57. J. Sakabe, N. Ohta, T. Ohnishi, K. Mitsuishi, and K. Takada, Commun. Chem., 1, 1 (2018).